Fate of intertidal microphytobenthos nitrogen under enhanced nutrient availability: Evidence for reduced nitrogen retention revealed through ^{15}N-labeling

Philip M Riekenberg[a,b *], Joanne M. Oakes[a], Bradley D. Eyre[a]

[a] Centre for Coastal Biogeochemistry, Southern Cross University, PO Box 157, Lismore, NSW 2480, Australia

[b] NIOZ, Royal Netherlands Institute for Sea Research and Utrecht University, Department of Marine Microbiology and Biogeochemistry, PO Box 59, Den Hoorn, 1790AB, Netherlands

[*] Corresponding author: phrieken@gmail.com

Keywords: ^{15}N, amino acid, denitrification, pulse-chase, intertidal, flood

Running head: Fate of microphytobenthos nitrogen

Abstract

Sediment microbial communities are an important sink for both organic and inorganic nitrogen (N), with microphytobenthos (MPB) biomass having the largest contribution to short-term N-assimilation and retention. Coastal waters are increasingly subject to anthropogenic nutrient enrichment, but the effect of this nutrient enrichment on microbial assimilation, processing, and fate of MPB-derived N (MPB-N) remains poorly characterized. In this study, an MPB community was labeled in situ with a pulse of $^{15}NH_4^+$-N. Laboratory core incubations of this labeled sediment under different nutrient concentrations (NH_4^+ and PO_4^{3-}: ambient, 2× ambient, 5× ambient, and 10× ambient) were used to investigate changes in the processing and flux pathways of the ^{15}N-labeled MPB-N across 10.5 d under nutrient enrichment. Initial production of MPB-N was stimulated by nutrient addition, with higher ^{15}N incorporation into MPB in the nutrient amended treatments (71-93%) than in the ambient treatment (38%). After 10.5 d, the nutrient amended treatments had increased turnover of MPB-N out of MPB biomass into an uncharacterized pool of sediment ON (45-75%). Increased turnover of MPB-N likely resulted from a decoupling between EPS production and bacterial remineralization as inorganic nutrients were preferentially used as an N source. This decoupling decreased the efflux of MPB-N via DON in the amended (3.9-5.2%) versus the ambient treatment (10.9%). Exports of MPB-N to the water column were relatively small, accounting for a maximum of 14% of ^{15}N exported from the sediment, and were dominated by export of DON and N_2 (denitrification). Overall, there was considerable retention of MPB-N over 10.5 d, but increased nutrient loading shifted N from MPB biomass into other sediment ON.

1 Introduction

Within shallow photic sediments, microphytobenthos (MPB) contribute significantly to primary production and biomass by fixing carbon (C) and utilizing nitrogen (N) from the water column and porewater (Dalsgaard, 2003; Ferguson et al., 2004; McGlathery et al., 2007). Coupling between MPB production and bacterial remineralization within these sediments can result in strong retention of N and recycling of C. Bacteria utilize the extracellular polymeric substances (EPS) produced by MPB, while MPB rely on inorganic sources or bacterially-excreted NH_4^+ from remineralization of organic matter (Cook et al., 2007; Forehead et al., 2013). The fate and processing of MPB-derived C (MPB-C) within sediments has been well described, with studies quantifying the incorporation of MPB-C into sediment organic matter and its loss from the sediment via efflux of dissolved organic carbon (DOC) and dissolved inorganic carbon (DIC) (Middelburg and Nieuwenhuize, 2001; Oakes et al., 2012; Oakes and Eyre, 2014; Oakes et al., 2016). Multiple studies have observed that respiration to DIC is the dominant pathway for MPB-C loss in coastal sediments while little MPB-C was exported as DOC (Oakes et al., 2012; Oakes and Eyre, 2014; Oakes et al., 2016). In contrast to MPB-C, the processing and fate of MPB-derived N (MPB-N) in coastal sediments is poorly understood, with only two comprehensive studies having quantified MPB-N incorporation into sediment compartments and its loss via sediment-water fluxes of dissolved inorganic nitrogen (DIN), dissolved organic nitrogen (DON) and dinitrogen (N_2) (Eyre et al., 2016). These studies quantified processing and loss of N via effluxes of DIN (37.3%, 1.9%, Eyre et al. 2016, Oakes et al., in press; respectively throughout), DON (12.6%, 0.5%) and N_2 during tidal inundation (20.7%, 0.9%), with only 27% and 12.4% (lower due to physical loss) of the initially incorporated ^{15}N retained within

the sediment after ~30 d. MPB dominated initial uptake of ^{15}N (50% and 75% MPB vs. 2% and 9% bacteria, respectively), but was only the dominant reservoir for MPB-N within sediment organic nitrogen (sediment ON) by day 23 in the subtidal study (80.4 % MPB, 2.7% bacteria, and 15.9% uncharacterized; Eyre et al., 2016). In the intertidal study, MPB and uncharacterized material contained comparable amounts of MPB-N by day 31 (50% MPB, 1.6% bacteria, and 48.4%, Oakes et al., in press). Increased turnover into the uncharacterized pool between these two studies may indicate quicker turnover of newly assimilated MPB-N into sediment ON in intertidal settings.

Coastal waters are increasingly subject to anthropogenic nutrient enrichment (Howarth and Marino, 2006) which alters biogeochemical pathways and can cause eutrophication within otherwise healthy estuaries (Howarth and Marino, 2006; Rabalais et al., 2009). Within intertidal sediments, increased availability of inorganic nutrients from anthropogenic sources is expected to alter the processing of MPB-N as the microbial community responds to an additional source of N that was previously in limited supply. Efflux of N as DIN or N_2 occurs as the net result of mineralization and competition between MPB, heterotrophic bacteria, and denitrifying bacteria for uptake of available NH_4^+. In N-limited settings, strong competition for nutrients arising from bacterial remineralization of sediment ON results in strong retention of remineralized MPB-N within sediment organic matter (OM) compartments (MPB, bacteria, and uncharacterized) (Fig.1A) and little N is available for export via DIN or the coupled nitrification-denitrification pathways (Cook et al., 2004; Cook et al., 2007; McGlathery et al., 2007; Sundback et al., 2000). With additional nutrient inputs stimulation of MPB productivity has been observed to coincide with decreasing efflux of DIN and N_2 to the water column (Dalsgaard, 2003; Ferguson and Eyre,

2013; Ferguson et al., 2004). Few studies have examined how increased N availability in the water column affects the processing and fate of MPB-N within shallow photic coastal settings. A laboratory study partitioned the algal and bacterial contribution to uptake of ^{15}N within the sediment microbial community through the use a biomarker technique (D/L-Alanine) and found that the addition of nutrients (NH_4^+, $Si(OH)_4$, HPO_4^-) increased MPB incorporation of ^{15}N and decreased competition for inorganic nutrients between MPB and bacteria (Cook et al. (2007); Fig. 1B). However, this study did not quantify water column efflux of DIN, DON or N_2.

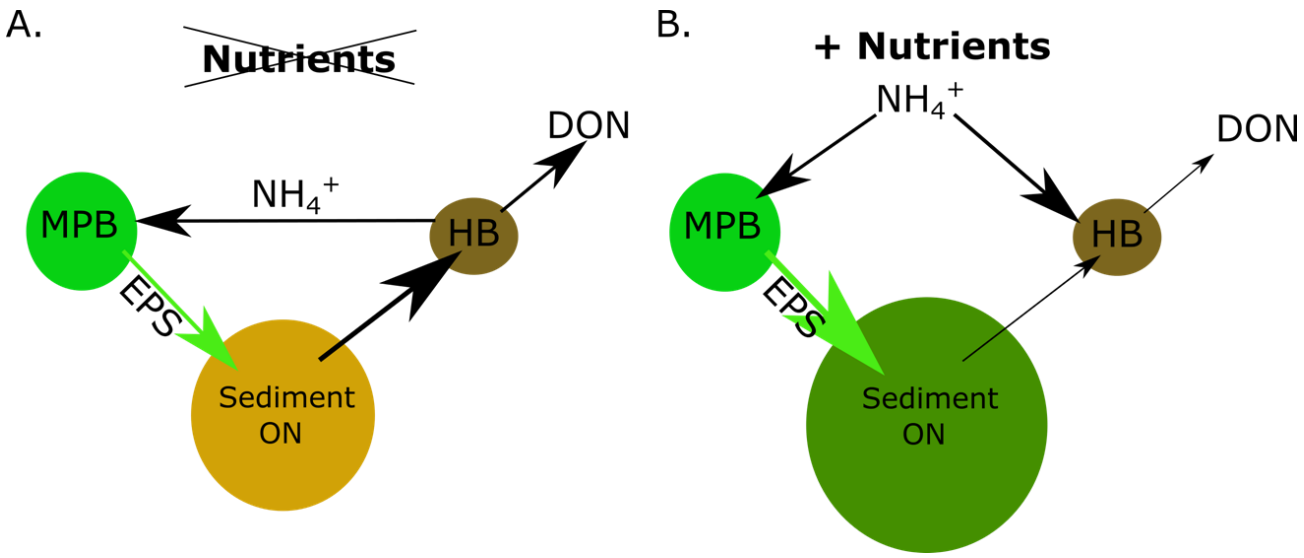

Figure 1: Conceptual diagram of the hypothesized mechanism and change in relationship between microphytobenthos (MPB) and heterotrophic bacteria (HB) under A) nutrient limiting and B) nutrient replete settings. A) When nutrients are scarce there is a strong coupling between bacterial remineralization of MPB-N within sediment ON and competition for nutrients between MPB and HB. Tight coupling results in significant turnover of MPB-N between the three sediment compartments and increased export of MPB-N as DON as EPS is remineralized. B) When inorganic nutrients are available, bacterial remineralization decreases as inorganic nutrients are preferentially used over sediment ON and results in decreased competition between MPB and HB for nutrients. Decoupling between HB remineralization of MPB-derived OM results in the buildup of MPB-N in sediment ON and decreased production of DON as remineralization is decreased.

In this ^{15}N pulse-chase study we aimed to quantify changes in the processing and fate of MPB-N within subtropical intertidal sediments due to increased water column nutrient availability. Pathways considered included transfer of MPB-N through sediment ON compartments (MPB, bacteria and uncharacterized), and export via efflux of NH_4^+, DON, and N_2 to the overlying water column. We expected decreased remineralization, re-capture, and recycling of processed MPB-N through the sediment compartments as introduced inorganic nutrients were preferentially utilized by the microbial community. This could result in either increased retention of MPB-N within the uncharacterized sediment organic matter pool due to decreased utilization by both MPB and bacteria, or increased MPB-N export as MPB-N is effluxed to the water column without being re-captured and recycled. As a result of decreased recycling of MPB-N within the microbial community, we expect that export of ^{15}N via efflux of NH_4^+, DON, and N_2 would be reduced as a result of increased sediment retention within N replete treatments (Fig. 1B).

2 Methods

2.1 *Study site*

The study site was a subtropical intertidal shoal ~2 km upstream of the mouth of the Richmond River estuary in New South Wales, Australia (28˚52'30"S, 153˚33'26"E) that was simultaneously used for a ^{13}C pulse-chase study (Riekenberg et al. 2018). The 6900 km^2 Richmond River catchment has a mean annual rainfall of 1300 mm (McKee et al., 2000) and an average flow rate of 2200 ML d^{-1} (daily gauged flow adjusted for catchment area, averaged over years for which data was available; 1970–2013). Although the Richmond River estuary has highly variable flushing, salinity, and nutrient concentrations associated

with frequent episodic rainfall events and flooding (Eyre, 1997; McKee et al., 2000), this study was undertaken during a period of average rainfall (~200 mm in the month prior). The site experiences semidiurnal tides with a range of ~2 m. Samples were collected in January 2015 (summer) with average site water temperature of 25.6 ± 2.3°C. Sediment at depths of 0-2 cm, 2-5 cm and 5-10 cm was dominated by fine sand (66%-73%) and sediment across 0-10 cm had an organic N content of 1.2 ± 0.1 mol N m^{-2}. Sediment molar C:N was lowest at 2-5 cm, but comparable across other depths (0-2 cm 17.2 ± 1.7, 2-5 cm 10.9 ± 0.5, 5-10 cm 16.2 ± 2.2). The MPB assemblage was dominated by pennate diatoms with few larger heterotrophs (>500 µM) and no cyanobacteria observed under light microscopy (1000 ×) as has been described previously for this site (Oakes and Eyre, 2014; Riekenberg et al., 2017; Riekenberg et al., 2018). Foraminifera were the dominant heterotrophs observed within site sediments, but were not considered in the current study, as they have previously been found to make only a minimal contribution to uptake of MPB-N (~1%) in sediments in the adjacent Brunswick Estuary (Eyre et al., 2016).

2.2 *Experimental overview*

An in situ application of ^{15}N (99% NH_4^+) was used to introduce a pulse of ^{15}N-labeled MPB-N into sediment. Unincorporated ^{15}N was flushed from the sediment during the next tidal inundation of the site. Sediment cores were then collected and incubated in the laboratory under four nutrient enrichment scenarios (ambient, minimal, moderate, and elevated) using pulsed nutrient additions. Laboratory incubation of cores allowed for explicit control of nutrient additions and was used to examine the fate and processing of the pulse of MPB-N over 10.5 d. Sediments remained inundated during incubation to minimize loss of MPB-N through physical processes as we were primarily interested in biological sediment

processing and previous studies have shown that physical loss processes can have an important seasonal role in the processing of MPB-N (Nielsen et al., 2017).

2.3 *^{15}N labeling*

An experimental plot (2 m^2) of bare sediment free of large animal burrows was labeled with ^{15}N (99% $^{15}NH_4^+$) when sediments were initially exposed during the ebbing tide in the middle of the day. To ensure even application, the plot was divided into 400 cm^2 subplots and a 20 ml aliquot of 40µmol $^{15}NH_4^+$ solution was sprayed onto each subplot using motorized sprayers. This gave a label application rate of 2 mmol $^{15}NH_4^+$ m^{-2}. The labeled solution was prepared with NaCl amended Milli-Q to match site salinity (34.6). Assimilation of ^{15}N by the sediment community occurred during the 4 h prior to tidal inundation. The tide then removed unincorporated ^{15}N; as confirmed by measurement of removal of ^{15}N from the initial application (90.3%) in 0-10 cm of sediment during initial sampling.

2.4 *Sample collection*

Prior to application of ^{15}N, 3 cores (9 cm diameter, 20 cm depth) were collected immediately adjacent to the treatment plot and were immediately extruded and sectioned (0-2 cm, 2-5 cm, and 5-10 cm) to provide unlabeled control samples for sediment ON $\delta^{15}N$. At the next low tide (11 h after label application), 43 sediment cores were collected from the labeled plot using clear acrylic core liners (9 cm diameter, 47 cm height). Immediately, three cores were extruded and sectioned, as described above. The sediment samples were placed into plastic bags, transported to the laboratory on ice, stored frozen in the dark (-20˚C), and were later used to determine initial ^{15}N uptake, grain size distribution across sediment depths, and chlorophyll-α (Chl-α) concentration within 0-1 cm sediments. The 40 remaining

core liners were sealed with acrylic bottom plates and transported to the laboratory for incubation within 2 h of sampling. Site water (400 L) was collected and transported to the laboratory for use during incubations.

2.5 *Nutrient Amendment*

Sediment cores were incubated in the laboratory with a range of nutrient concentrations in the overlying water that were below the sediment capacity for uptake. Incubation tanks (85 L volume), each containing ten cores, were established with nutrients at ambient concentration (site water: DIN of 2.5 ± 0.04 µM N L^{-1}, TP 0.9 ± 0.09 µM P L^{-1} measured on incoming tide), and with N (NH_4^+) and P (H_3PO_4) amendments to site water at 2× (minimal treatment), 5× (moderate treatment), and 10× (elevated treatment) average water column concentrations near the study site (4 µM L^{-1} NH_4^+ and 5 µM L^{-1} PO_4^{3-}, Eyre (2000)). Nutrient amendments were added to the incubation tanks and to bags of replacement water an hour prior to cores being transferred into treatment tanks for incubation. Two additional identical amendments of NH_4^+ were added to maintain the respective treatment concentrations to the incubation tanks after sampling at 1.5 d and 3.5 d of incubation to ensure that nutrient limitation did not develop after uptake of the initial treatment addition (Appendix Fig. 1). There was no significant accumulation of NH_4^+ within treatment tank waters, as nutrients were readily processed and removed from the water column within 24 h of additions. An addition of sodium metasilicate (Na_2SiO_3, 17 µmol Si L^{-1}) was also added to all incubation tanks at the end of the 2.5 d of incubation to prevent secondary limitation of Si.

2.6 *Benthic flux incubations*

198 In the laboratory, cores were fitted with magnetic stir bars positioned 10 cm above
199 the sediment surface, filled with ~2 L of site water, and randomly allocated to one of the four
200 treatment tanks (ambient, minimal, moderate, elevated; ten cores per treatment). Water
201 within treatment tanks and cores was continuously recirculated, held at in situ temperature
202 ($25 \pm 1^{o}C$) using a temperature controller, and aerated. Cores were stirred at a rate below the
203 threshold for sediment resuspension (Ferguson et al., 2003) via a rotating magnet at the
204 center of each treatment tank, which interacted with the magnetic stir bars. Three sodium
205 halide lamps suspended above the treatment tanks approximated the average light level
206 measured at the sediment surface during inundation (941.4 ± 139 µE m^{-2} s^{-1}) by providing
207 824 ± 40 µE m^{-2} s^{-1} to the sediment/water interface within the cores on a 12 h light/12 h dark
208 cycle. Cores were allowed to acclimate in the treatment tanks for 6 h prior to the start of
209 incubation, allowing sediment microhabitats to re-establish. Cores remained open to the tank
210 water until 30 min before sampling when clear Plexiglas lids were fitted to each core liner to
211 seal in overlying water within the core for the duration of the incubation (~16 h). On each
212 sampling occasion, 8 cores (2 per treatment at 1.5, 2.5, 3.5 and 10.5 d) were sampled for
213 dissolved oxygen (± 0.01 mg/L) and temperature ($\pm 0.01^{\circ}C$) using a Hach HQ40d multi-
214 parameter meter via a sampling port in the core lid. For each sampling period, measurements
215 were made at three time points (initial, dark end/light start, and light end) to allow dark,
216 light, and net flux calculations. Initial samples were taken 30 min after closure of the lids,
217 dark end/light start samples were taken after ~12 hours incubation with no light, and light
218 end samples were taken 3 hours after illumination at the end of the dark sampling. At each
219 initial, dark end/light start, and light end sampling duplicate samples for N_2:Ar analysis were
220 collected by allowing water from suspended replacement water bags to gently displace

sample water out of the core via tubing into 7 ml gastight glass-stoppered glass vials. These vials were allowed to overflow by 2-3 volumes, killed with 20 µl of saturated $HgCl_2$ and stored submerged at ambient temperature. To determine NH_4^+, NO_3^-, and DON concentrations and $\delta^{15}N$ values, sample water was syringe-filtered (0.45 µm cellulose acetate) into 10 ml and 50 ml polyethylene vials, leaving a headspace, and stored frozen (-20°C). To determine $\delta^{15}N$ values for N_2, sample water was filtered (0.45 µm cellulose acetate) into a 20 ml glass vial containing 500 µl of 2M NaOH. These samples were sealed without headspace using a lid containing a teflon-coated septum and refrigerated for storage. After completion of the dark/light flux incubation, cores were sacrificed and sediment was extruded and sectioned (top scrape, 0.2-2 cm, 2-5 cm, and 5-10 cm depths). A subsample (1 cm^3) of sediment was taken for Chl-α analysis from the 0-1 cm depth prior to sectioning of the 0-2 cm layer using a spatula and placed in a 10 ml centrifuge vial containing 5 ml of 90% acetone. Sediment samples were placed in ziplock bags and stored in the dark at -20°C until analysis.

2.7 *Sample analysis*-

A portion of each sediment sample was freeze-dried and KCl-extracted (2M KCl) for analysis of concentration and $\delta^{15}N$ of sediment ON. Both washed (KCl-extracted) and raw (non KCl-extracted) sediment samples were dried (60°C) and weighed into tin capsules for analysis of $\delta^{15}N$ and %N using a Flash elemental analyzer coupled on-line to a Thermo Fisher Delta V Plus isotope ratio mass spectrometer (IRMS). Reproducibility of $\delta^{15}N$ values for samples with $\delta^{15}N$ enrichment <100‰ was ± 0.2‰. Precision decreased with enrichment beyond 100‰. Additional freeze-dried sediment was analyzed for D- and L- alanine

concentration and $\delta^{15}N$ to determine the relative contribution to uptake of ^{15}N by both MPB and bacteria, as described below.

N_2 concentrations were analyzed using N_2:Ar measured with a membrane inlet mass spectrometer with O_2 removal (Eyre et al., 2002). Concentrations for DON, NH_4^+, and NO_3^- were determined through colorimetric analysis on a four channel Flow Injection Analyzer (FIA, Lachat QuickChem 8000) (Eyre et al., 2011). DON was quantified via measurement of total nitrogen (TN) through flow injection analysis using persulfate digestion (Valderrama, 1981) and subsequent subtraction of DIN ($NH_4^+ + NO_3^-$) concentrations (Lachat, 1994). Prior to analysis, vials for N_2 analysis had 4 ml of water displaced with a helium headspace and were held at ambient temperature. $\delta^{15}N_2$ concentration of the He headspace in N_2 samples was determined via gas chromatography isotope ratio mass spectrometry using a Thermo Trace Ultra Gas Chromatograph coupled to a Delta V Plus IRMS via a Thermo Conflo III interface.

$\delta^{15}N$ for NH_4^+ was measured for samples with a concentration of >0.5 µmol N L^{-1} (as determined by Flow Injection Analyis) via chemical conversion of NH_4^+ to NO_2^- followed by azide conversion of NO_2^- to N_2O (Zhang et al., 2007). Samples with a concentration <0.5 µmol N L^{-1} were below the detection limit for this method and were assumed to contribute a negligible amount of $\delta^{15}N$ for calculations of MPB-N efflux. Concentrations of NO_3^- were consistently below the detection limit (0.5 µmol N L^{-1}) for the dentrifier method (Sigman et al., 2001) for the analysis of $^{15}NO_3^-$; NO_3^- was assumed to have a minimal contribution to the efflux of MPB-N. The isotopic composition of DON was determined after persulfate oxidation of TN to NO_3^-, followed by conversion to N_2O using the denitrifier method. The $\delta^{15}N$-DON was calculated using a two source mixing model based on $\delta^{15}N$ of TN and

266 $^{15}NH_4^+$ for samples with sufficient concentrations (Erler et al., 2014). Where NH_4^+
267 concentrations were <0.5 µmol N L^{-1}, no correction was applied and δ^{15}N-TN was used as
268 δ^{15}N-DON. NO_3^- was not considered in this calculation because it was consistently below
269 0.5 µmol N L^{-1} while DON concentrations were ~18 µmol N L^{-1} (~36 × greater).

270 The relative contribution of MPB and bacteria to ^{15}N uptake and transfer was
271 determined through compound-specific analysis of D- and L- alanine following acid
272 hydrolysis and extraction of total hydrolysable amino acids from 7 g of freeze-dried
273 sediment. Due to the laborious extraction process, only single replicates from the 0.2-2 cm,
274 2-5 cm and 5-10 cm depths of each core at each time were analyzed. Extraction and analysis
275 was performed as described by Veuger et al. (2005) and Veuger et al. (2007a), with minor
276 modifications. Briefly, freeze-dried sediment (7 g) was rinsed with 2 M HCl, centrifuged (5
277 min, 900 *g*), and the supernatant discarded. This was repeated with milli-Q water 3×, and the
278 sediment pellet was then hydrolyzed with 6 M HCl (110°C, 20 h). After hydrolysis, a
279 standard spike of L-norleucine (2.5 mg ml^{-1}) was added and the sample shaken and
280 centrifuged again. The supernatant was removed and retained. The pellet was then
281 resuspended in 10 ml milli-Q water, centrifuged 2×, and the additional supernatant also
282 retained. The combined supernatant (25 ml) was purified through cation exchange
283 chromatography (Dowex 50WX8-100), and the amino acids were derivatized with
284 isopropanol and penta-fluoropropionic anhydride, and further purified via solvent extraction
285 with chloroform. Concentrations and δ^{15}N of the derivatized amino acids were determined
286 via gas chromatography-combustion-isotope ratio mass spectrometry (GC-c-IRMS) on a HP
287 6890 GC interfaced via a Thermo Conflo III interfaced with a Thermo Delta V Plus IRMS
288 using the column and ramp schedule described in Eyre et al. (2016).

289 Chl-α was extracted by adding a 9/1 acetone/water mix followed with sonication (15
290 min), centrifugation (5 min, 9 *g*), and removal of the supernatant for analysis by colorimetry
291 (Lorenzen, 1967). ON within bulk sediment was analyzed for $\delta^{15}N$ after KCl-extraction to
292 remove any N adsorbed to sediment particles. Briefly, 2 g of homogenized freeze-dried
293 sediment were combined with 5 ml of 2M KCl in a centrifuge tube, shaken for 5 min, and
294 centrifuged (15 min, 9 *g*). The supernatant was discarded, and three times thereafter 5 ml of
295 milli-Q was added to the pellet prior to shaking (5 min), centrifugation (15 min, 9 *g*), and
296 removal of the supernatant. The KCl-extracted pellet was dried at 60°C to constant weight
297 and weighed into a tin capsule for analysis of $\delta^{15}N$ and %N using a Flash elemental analyzer
298 coupled on-line to a Thermo Fisher Delta V Plus IRMS. Reproducibility of $\delta^{15}N$ for samples
299 with enrichment < 100 ‰ was ± 0.2 ‰. Precision decreased with enrichment beyond 100
300 ‰.

301 2.8 *Calculations*

302 The total ON mass (biomass) of sediment was calculated as the product of %N and
303 dry mass of sediment per unit area. Incorporation of ^{15}N into sediment ON, bacteria and
304 MPB (mmol ^{15}N m^{-2}) was calculated as the product of excess ^{15}N (fraction ^{15}N in sample –
305 fraction ^{15}N in control) and the mass of ON within each pool.

306 Biomass and excess ^{15}N contained in bacteria and MPB was estimated based on the
307 excess ^{15}N contained within the amino acids D- and L- alanine (Ala). The assumptions and
308 uncertainty associated with this method are discussed in detail by Veuger et al. (2005) and
309 Veuger et al. (2007b) and estimates of error propagation for individual variables are
310 provided in Riekenberg et al. (2017). During acid hydrolysis, some racemization of L- Ala to

D- Ala occurs, resulting in a D- : L- Ala ratio of 0.015-0.02 for algal cultures (Veuger et al., 2007b) and 0.006 for dissolved free amino acids (Kaiser and Benner, 2005). In the current study, uncorrected D/L-Ala ratios as low as 0.009 were observed, and therefore a racemization rate of 0.006 was applied to correct for L-Ala racemization. This value corresponded well to measured values for racemization of L-Ala standards during hydrolysis under laboratory conditions. Measured D- and L- Ala concentrations were corrected for racemization using the equations of Kaiser and Benner (2005):

1. $L^*_0 = (L^* - D^* (0.6)) / 100 - 0.6$

2. $D^*_0 = D^* + L^* - L^*_0$

where L^*_0 and D^*_0 and L^* and D^* are the concentrations of L- and D-Ala occurring originally and after hydrolysis, respectively. Original concentrations of D- and L-Ala represent concentrations of both forms of alanine derived from bacterial and algal biomass prior to hydrolysis induced racemization.

Biomass of heterotrophic bacteria (HB), MPB, and total microbial biomass were calculated as described by Veuger et al. (2005) and Veuger et al. (2007b), as follows:

3. HB L-Ala = D^*_0-Ala × 20

4. HB contribution to microbial biomass (%) = (HB L-Ala / L^*_0-Ala) ×100

5. MPB contribution to microbial biomass (%) = 1 – HB contribution to microbial biomass

6. HB biomass = D^*_0-Ala × 400

where 20 is the conversion for excess ^{15}N in D-Ala (5%) that represents excess ^{15}N present in bacterial L-Ala (20×). This conversion factor is based on culture analysis (Veuger et al.,

2005; Veuger et al., 2007b), is further discussed in Eyre et al. (2016), and assumes a negligible contribution of Gram positive bacteria or cyanobacteria to the benthic community. The lack of cyanobacteria in the current study was confirmed through both microscope work and PLFA analysis (Riekenberg et al. 2018). The conversion factor of 400 (Veuger et al., 2005) accounts for the % N in dry bacterial biomass (12%; (Madigan et al., 2000), and yields a D-Ala content of 0.25. ^{15}N uptake into HB, MPB, and total microbial biomass were calculated using equations 3-8, substituting excess ^{15}N values for L^*_0- and D^*_0-Ala in place of L^*_0- and D^*_0-Ala contents.

Total excess ^{15}N within water column NH_4^+, DON and N_2 were calculated for the beginning and end of dark incubation period and the end of the light incubation period as the product of excess ^{15}N in NH_4^+, DON and N_2 (excess $^{15}N_{sample}$ – excess $^{15}N_{control}$), core volume, and concentration of NH_4^+, DON, and N_2. Total excess flux of ^{15}N in NH_4^+, DON, and N_2 was calculated as:

7. Excess ^{15}N flux = (Excess $^{15}N_{start}$ – Excess $^{15}N_{end}$) / SA / t

where excess $^{15}N_{start}$ and excess $^{15}N_{end}$ represent excess ^{15}N in NH_4^+, DON, and N_2 at the start and end of the dark and light incubation period, SA is sediment surface area, and t is the incubation period (h) in the light or the dark. Net flux of excess ^{15}N (excess ^{15}N m^{-2} h^{-1}) for NH_4^+, DON, and N_2 was calculated as:

8. Net flux = (dark flux * dark hours) + (light flux * light hours) / 24 h

export of ^{15}N to the water column via $^{15}NH_4^+$, $DO^{15}N$, and $^{15}N_2$ was estimated through interpolation between efflux measurements for each treatment by calculation of the area beneath the curve during each sampling period. Incubations for dark periods were ~12 h while light periods were limited to ~4 h as required to prevent supersaturation and bubble

development samples taken to measure N_2/Ar for N_2 fluxes. Fluxes of excess $^{15}NO_3^-$ were assumed to be negligible and were therefore not included in excess flux measurements for DIN because core water column concentrations were consistently low and below the detection limit required for analysis of $\delta^{15}N$ values via the denitrifier method (0.5 uM N L^{-1}; Sigman et al. (2001).

2.9 *Data Analysis*

In the initial sampling period, there was incorporation of MPB-N below 2 cm (2-10 cm) within all of the treatments. A one-way analysis of variance was used (ANOVA) to determine whether there was a significant difference amongst treatments ($\alpha = 0.05$). A one-way ANOVA was also used to determine if there was a significant difference among treatments in ^{15}N uptake into MPB during the initial sampling period. Levene's tests indicated that variances were homogenous in all cases. When significant differences were indicated, post-hoc Tukey tests investigated the differences between treatments ($\alpha = 0.05$).

Two-way ANOVAs were separately applied to Chl-α and ^{15}N incorporation with pooled depths of 0-2 cm and 2-10 cm across sampling times to determine whether significant differences occurred between treatments or depths within each time period. Additional two-way ANOVAs were used to investigate whether significant differences occurred between sediment compartments (uncharacterized, MPB, and bacteria) within ambient or nutrient amended treatments. Levene's tests indicated that variances were homogenous in all cases, and there were no significant interactions indicated during these analyses. Where ANOVAs indicated a significant difference ($\alpha = 0.05$), post-hoc Tukey tests were applied to investigate significant differences between variables ($\alpha = 0.05$).

3 Results

3.1 *Sediment characteristics*

Sediment Chl-α at 0.2-2 cm depth averaged 48.3 ± 2.9 mg m^{-2} (mean ± SE) across all cores collected in this study and was not affected by time or treatment (two-way ANOVA: $F_{3,20}$=0.8, p=0.5). Sediment organic matter across the 0-10 cm depth had a molar C:N ratio of 18.1 ± 1.1 and contained 1.2 ± 0.1 mol N m^{-2}. The %N of sediment was low and even across all sediment layers (0.02%). Within initial cores taken after labeling, but prior to incubation, MPB biomass had the greatest contribution to sediment ON (20%) in the 0-2 cm depth, with bacteria representing only 4% (Table 1). Due to uptake of ^{15}N being largely confined to ON in the uppermost sediment layer (0-2 cm) in the initial cores, deeper depths (2-5 cm and 5-10 cm) were not examined for uptake into MPB, bacteria, and uncharacterized sediment compartments. Within the ambient treatment across samplings, MPB had the greatest contribution to ON in the uppermost layer (0-2 cm, 28.4%) and contributed less in deeper depths (2-5 cm, 10.7%; 5-10 cm, 6.4 %, Table 1). Bacterial contribution to ON was less than MPB in the uppermost layer (0-2 cm, 17.4%) and decreased with depth (2-5 cm, 7.1%; 5-10 cm, 6.0%). Uncharacterized ON made the largest contribution to both initial (75%) and ambient (54-88%, Table 1) sediments within this study.

	0-2 cm			2-5 cm			5-10 cm		
	mmol N m^{-2}	SE	%N	mmol N m^{-2}	SE	%N	mmol N m^{-2}	SE	%N
Initial									
Sediment	268.3	19.1	21.2	465.7	29.7	36.9	529.7	44.7	41.9
MPB	53.8	3.1	20.1						
Bacteria	11.1	0.0	4.1						
Uncharacterized	201.6	36.1	75.1						
Ambient									
Sediment	231.1	18.8	19.8	421.4	93.3	36.1	515.7	73.3	44.1
MPB	65.6	8.1	28.4	45.2	10.5	10.7	33.2	13.2	6.4
Bacteria	40.3	10.5	17.4	29.8	4.6	7.1	31.1	7.3	6.0
Uncharacterized	125.2	23.0	54.2	346.4	94.0	82.2	451.3	74.9	87.5

Table 1: Mean biomass for sediment compartments for 0-2 cm for initially sampled cores after tidal flushing and for 0-2 cm, 2-5 cm, and 5-10 cm for all cores sampled in the ambient treatment (mean ± SE). %N is the percentage N within each sediment depth for individual sediment compartments (MPB, Bacteria, and Uncharacterized) except for sediment N, where it represents the portion of N relative to the total N in 0-10 cm of sediment.

3.2 *Uptake of ^{15}N*

The pulse of ^{15}N was rapidly incorporated into sediment ON, with 193 ± 44.8 µmol ^{15}N m^{-2} detected in 0-2 cm of sediment 11 h after label application, when the first ^{15}N-labeled cores were collected after tidal flushing. At 0-2 cm, ^{15}N uptake into the microbial community was dominated by MPB (MPB 53.8 mmol N m^{-2}, 83%; bacteria 11.1 mmol N m^{-2}, 17%, Table 1). At this time ^{15}N was largely confined to the top scrape (upper 2 mm of sediment) and 0-2 cm depths (84.8 mmol N m^{-2}, 43.8% and 85.4 mmol N m^{-2}; 44.1% of total incorporated ^{15}N, 193.4 mmol N m^{-2}, respectively), but some downward transport of ^{15}N was evident in the 2-5 cm and 5-10 cm depths (10.2 mmol N m^{-2}, 5.3%; 13.1 mmol N m^{-2}, 6.8%, respectively). Due to limited labeling uptake within the lower depths during the initial sampling, we did not run D/L-Ala analysis for the microbial community in the 2-5 cm and 5-10 cm depths.

415 ^{15}N was incorporated into deeper sediments (2-5 cm and 5-10 cm) within all
416 treatments by the initial sampling time (Fig. 2). By 0.5 d, comparable amounts of the
417 assimilated MPB-N (8-16%) was in sediment below 2 cm (One-way ANOVA: $F_{3,7}$=5.3,
418 p=0.07, ambient 12%; minimal 16%; moderate 8%; and elevated 10%). After 10.5 d there
419 was significantly more ^{15}N contained in the 0-2 cm layer (TS + 0.2-2 cm) than the 2-5 cm or
420 5-10 cm layers across all treatments (two-way ANOVA: $F_{2, 108}$ =1070, p<0.001; Fig. 2;
421 ambient 83.4%, minimal 81.9%, moderate 79.1%, and elevated 78.6%). Tukey tests
422 indicated that incorporation into the 2-5 and 5-10 cm depths were similarly low for all
423 treatments across sampling times.

424 Uptake of ^{15}N into microbial biomass (MPB and bacteria) accounted for 22-95% of
425 the total ^{15}N incorporated into sediment ON across all treatments and sampling times (Fig.
426 3). Initial ^{15}N contained (0.5 d) in MPB during the incubation was higher in the elevated
427 treatment (one-way ANOVA: $F_{3,7}$=6.9, p=0.046, minimal, 71±21% ; moderate, 75±12%;
428 and elevated, 93±1%, mean±SE) than in the ambient treatment (38±4%) with Tukey tests
429 indicating a significant difference between elevated and ambient treatments (p=0.04) with
430 values for minimal and moderate treatments falling intermediate between them. This
431 indicates that initial production of MPB-N was stimulated by increased nutrient availability
432 and remained in MPB at 0.5 d. Within the microbial community after 0.5 d, distribution of
433 ^{15}N continued to be dominated by MPB for all treatments (ambient 83±3%; minimal 79±4%;
434 moderate 74±2%; elevated 75±5%, Fig. 4). Bacterial contribution to ^{15}N uptake was
435 comparable or higher during the later sampling times (1.5 to 10.5 d) in the nutrient amended
436 treatments (minimal, 15-23%; moderate, 2-49%; elevated, 2-40%, Fig.15) compared to the
437 ambient treatment (10-23%).

In the ambient treatment, distribution of ^{15}N between microbial biomass and uncharacterized sediment ON remained comparable across the 10.5 d incubation (one-way ANOVA: $F_{4,9}$ =0.5, p =0.8; Fig.14). In contrast, in the nutrient amended treatments ^{15}N incorporation was initially dominated by microbial biomass, primarily MPB, but shifted towards increased incorporation into the uncharacterized pool as the incubations progressed (two-way ANOVAs: minimal, $F_{1, 10}$ =10, p=0.01; moderate, $F_{1, 10}$ =10, p<0.001; elevated, $F_{1, 10}$ =10, p<0.001; Fig. 3). In the nutrient amended treatments, the ^{15}N contributing to the increased uncharacterized pool appeared to be largely sourced from MPB, resulting in reduced MPB contributions by 10.5 d (minimal 38%; moderate 12%; elevated 16%; Fig. 3). Bacterial contributions to ^{15}N remained comparable across the incubation period in nutrient amended treatments (two-way ANOVA: $F_{2, 15}$ =0.1, p =0.9).

3.3 *Loss of ^{15}N from sediments*

There was relatively little efflux of ^{15}N from the sediment to the water column in this study, with loss pathways accounting for a maximum of 14% of the initially incorporated ^{15}N across treatments (Fig. 2). Across all treatments, most of this loss to the water column occurred in the form of DON and N_2 fluxes (Fig. 5), with only a minor contribution from DIN (NH_4^+, maximum of 0.3%). Within the ambient treatment, DON was the largest export pathway accounting for loss over 10.5 d of 10.5% of the initially incorporated ^{15}N (Fig. 5 & 6). Loss of ^{15}N from the sediments via DON effluxes was lower within the nutrient amended treatments (minimal, 4.8%; moderate, 5.2%; elevated, 5.2%) but was not statistically significant. Export of ^{15}N via N_2 was comparably low between ambient, minimal and elevated treatments (3.3%, 2.8%, and 2.3%, respectively), but was higher in the moderate treatment (7.1%, Fig. 4 & 6). Overall export via combined efflux pathways was low across

all treatments, with the bulk of MPB-N remaining within the sediment by 10.5 d (ambient 86 ± 4%, minimal 90 ± 2%, moderate 88 ± 2%, and elevated 94 ± 3%, Fig. 6). The majority of ^{15}N remaining in the sediment was found in the 0-2 cm depth for all treatments (ambient 70%; minimal 63%; moderate 69%; and elevated 80%, Fig.2 while ^{15}N incorporation remained lower for depths below 2 cm (ambient 16%; minimal 27%; moderate 18%; and elevated 14%).

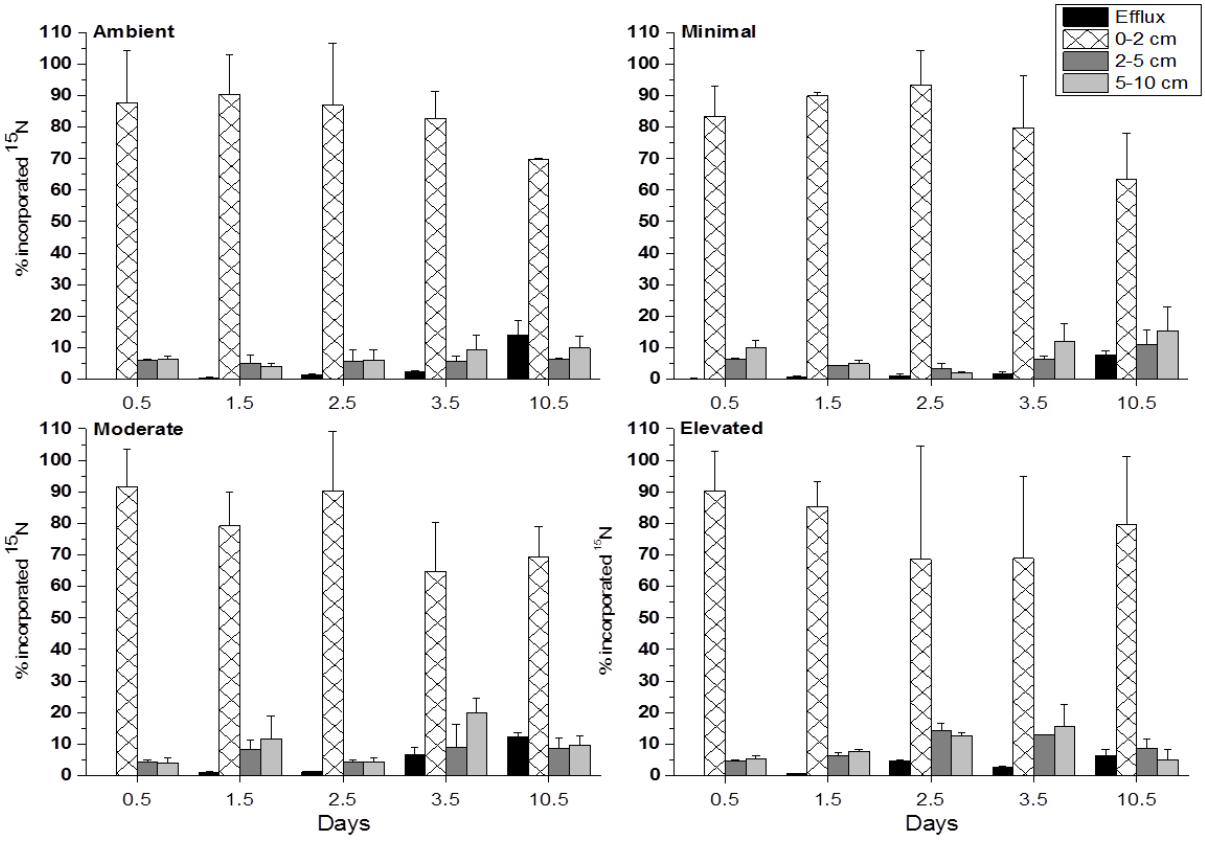

Figure 2: Nitrogen budget for excess ^{15}N within sediment ON at 0 to 2 cm, 2 to 5 cm, and 5-10 cm, and cumulative excess ^{15}N exported to the water column combined via effluxes of NH_4^+, DON, and N_2 for each treatment at each sampling time. All values are as a percentage of the ^{15}N initially incorporated into sediment ON (0-10 cm). Some error bars are too small to be seen (mean + SE).

4 Discussion

By combining a pulse-chase application of the rare isotope ^{15}N with the D/L-Ala biomarker technique, we identified that increased nutrient availability as a pulsed addition of 5 to 50 µM L^{-1} NH_4^+ across 3 treatments: 1) stimulated initial production of MPB-N 2) increased microbial turnover of MPB-N into the uncharacterized sediment ON compartment, and 3) decreased the amount of MPB-N lost via DON effluxes. By the end of the incubation (10.5 d) 86-94% of the ^{15}N incorporated remained in the sediment, with 3.9 - 10.9% effluxed as DON, 2.3 -7.1% effluxed as N_2, and less than 1% effluxed as NH_4^+ (Fig. 6). Of the ^{15}N contained in the sediment 12-40% was in MPB, 6-15% was in bacteria and the remaining 45-75% was uncharacterized (Fig. 6). This study is the first to track the fate and processing of a pulse of MPB-N produced in situ under an increasing gradient of water column nutrient availability.

4.1 *Initial incorporation and downward transfer of ^{15}N*

Initial uptake of ^{15}N into microbial biomass was dominated by MPB across all treatments (0.5 d, Fig. 4) and increased nutrient amendment stimulated initial retention of MPB-N within MPB (ambient 53% versus 84-95% nutrient amended treatments, 0.5 d, Fig. 3). Retention of MPB-N may have resulted from the decoupling of bacterial processing from MPB-N production, with inorganic nutrients preferentially utilized in lieu of MPB-N in the nutrient amended treatments. Decoupling is further supported by a decrease in MPB-N turnover into uncharacterized ON; there was the considerable initial turnover of MPB-N into the uncharacterized ON in the ambient treatment (47.3%, 0.5 d), but turnover within the nutrient amended treatments (5-16%, Fig. 3) was considerably lower (t= 3.8, p= 0.009). The

495 uncharacterized pool represents ^{15}N within bulk sediment OM that was not accounted for by
496 ^{15}N contained within microbial biomass. This pool is composed of ^{15}N-containing
497 compounds such as EPS, enzymes, and OM derived from the remineralization of MPB-N.
498 Increased breakdown and initial transfer of MPB-N into the uncharacterized pool is
499 consistent with increased bacterial utilization of MPB-N during remineralization that
500 resulted in increased initial turnover in low nutrient settings (Fig. 3). Increased coupling
501 between MPB and bacteria in low nutrient settings (Cook et al., 2007; Oakes et al., 2012)
502 has previously been attributed to increased reliance on the limited nutrients arising from
503 bacterial remineralization.

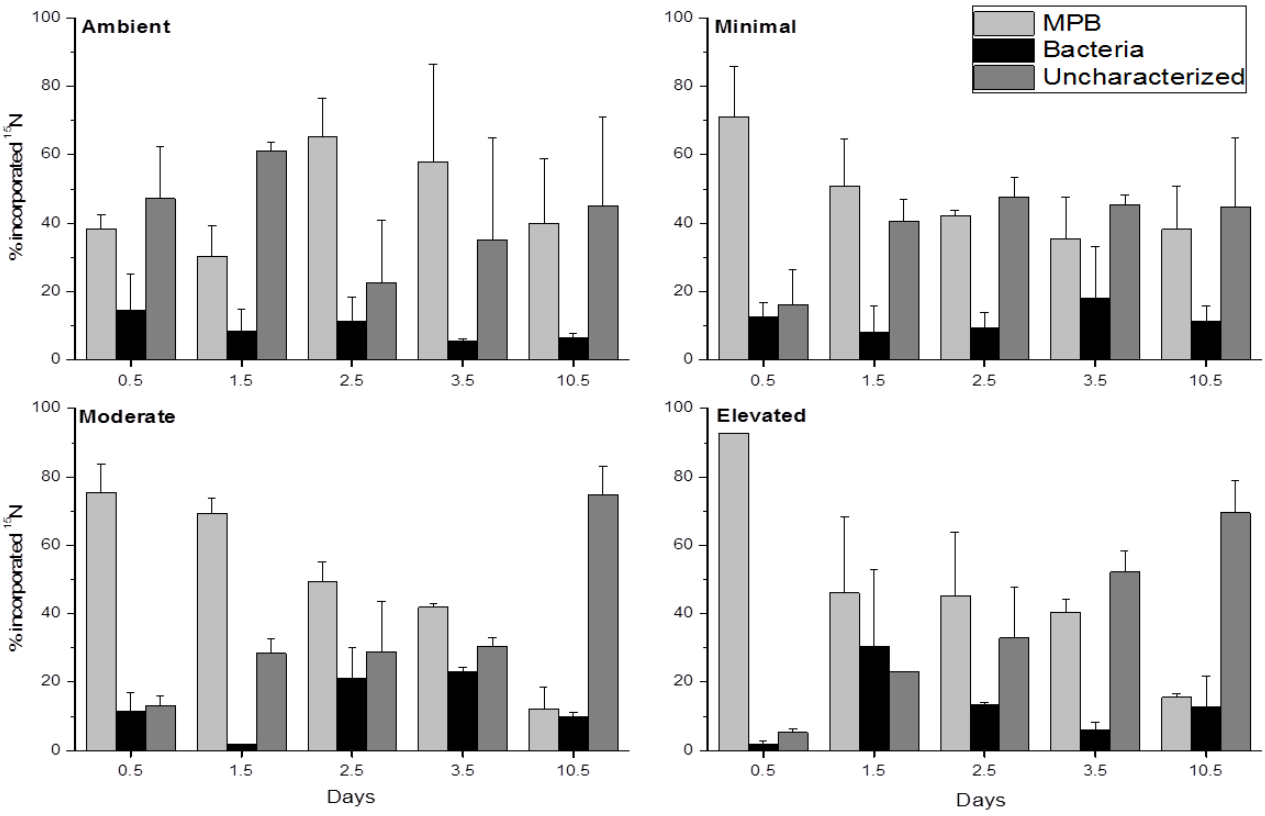

504

505 **Figure 3: Incorporation of ^{15}N into bacteria, MPB, and uncharacterized sediment**
506 **compartments (mean + SE). The uncharacterized compartment is derived by**
507 **subtracting ^{15}N contained in microbial biomass from bulk sediment organic ^{15}N.**

508

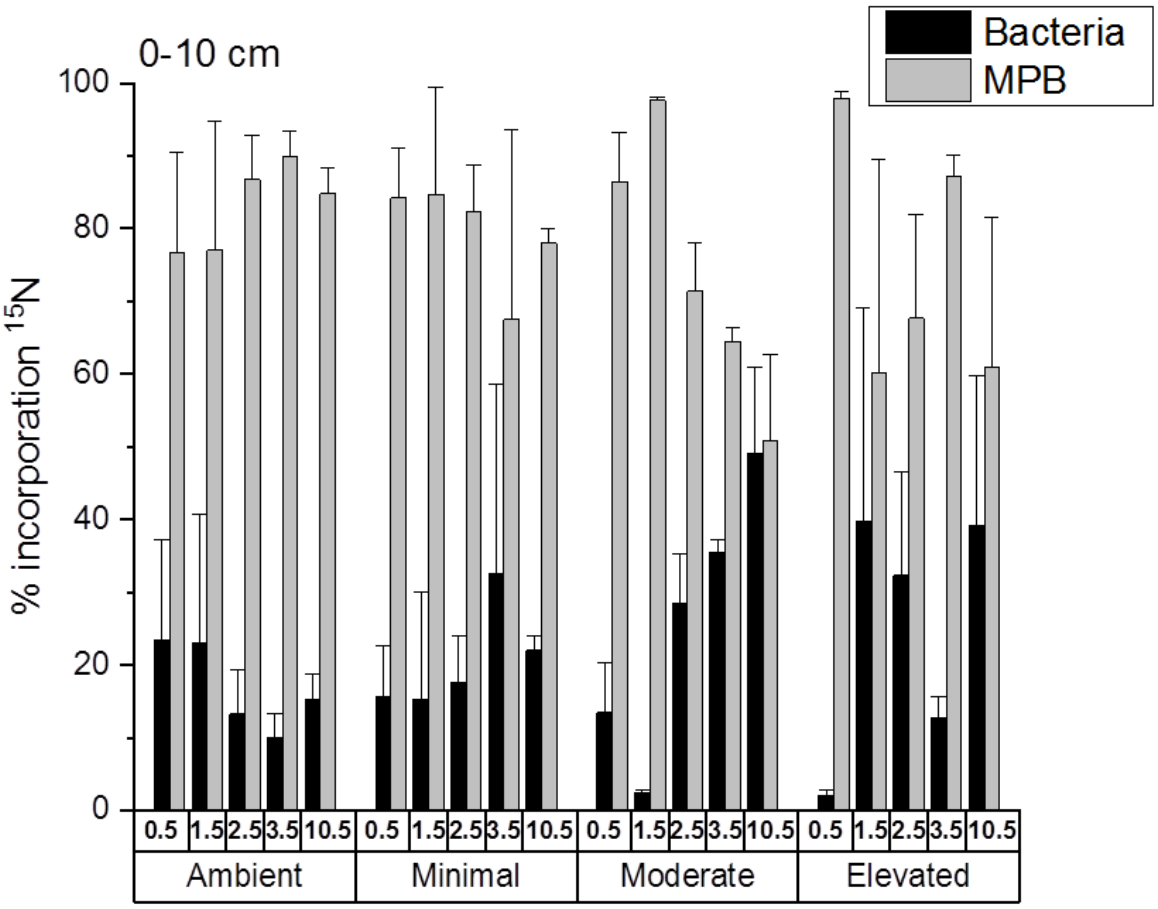

509

510 **Figure 4: Excess ^{15}N incorporation into MPB and bacterial biomass within 0-10 cm**
511 **depth as a percentage of the total ^{15}N incorporated into the microbial community for**
512 **each treatment at each time period (mean + SE).**

513 Ratios of ^{13}C:^{15}N uptake into microbial biomass were estimated based on the excess
514 ^{13}C incorporation determined in a complementary study (Riekenberg et al., 2018). Due to
515 phospholipid fatty acid analysis only accounting for the ^{13}C contained in living biomass and
516 D/L-Ala accounting for ^{15}N in both living and dead biomass, this ^{13}C:^{15}N ratio potentially
517 over-estimates the relative uptake of ^{15}N into the microbial community, particularly as

incubations progress. Therefore, we only considered the ^{13}C:^{15}N ratios for microbial biomass during the initial sampling (0.5 d) and not for subsequent samplings. The ^{13}C:^{15}N ratio in the ambient treatment (16.7±2.8) was considerably higher than in the nutrient amended treatments (minimal 8.3±3.8; moderate 5.2±3.4, and elevated 7.5±2; One-way ANOVA, $F_{3,7}$=5.4, p=0.068), and aligns well with previous estimates where preferential excretion of fixed C as EPS would occur due to N limitation within algal cells (e.g., ~20, Van den Meersche et al. (2004). The lower ^{13}C:^{15}N ratios within nutrient amended treatments indicate uptake occurring at a ratio closer to that of the Redfield ratio expected for algal uptake (6.7) as a result of increased N availability (Cook et al., 2007). The current study suggests that under N replete conditions, bacteria will utilize inorganic nutrients that are present to support production of low C:N biomass regardless of the C:N ratio of the substrate being processed to produce that biomass, as has been previously proposed (Goldman and Dennett, 2000).

Over 10.5 d, the majority (81%) of the ^{15}N incorporated into the sediment was recovered from the 0-2 cm depth, but incorporation of ^{15}N into deeper sediment layers occurred rapidly (within 0.5 d, Fig. 2), equating to a transport rate of ^{15}N to sediment below 2 cm of 2.7 – 4.4 μmol ^{15}N m^{-2} h^{-1}. This rate of downward transport was substantially lower than previously observed at this site (e.g., 19.6 μmol ^{15}N m^{-2} h^{-1} over 1.5 d, Oakes et al., in press) which may have been driven by the draining and re-filling of cores to simulate intertidal conditions in that study resulting in additional transport. The rates of downward transport for ^{15}N in this study are similar to that observed for MPB-N in subtropical subtidal sediments (e.g., ~2.7 μmol ^{15}N m^{-2} h^{-1} over 3 d with ambient DIN of ~8 μmolL^{-1}, Eyre et al. (2016), but represent a smaller portion of the total incorporated ^{15}N (8.3 – 16.4% compared to ~29%). The similar rates of downward transport for MPB-N between the two studies

likely reflect comparable downward migration by MPB within subtropical sands (Saburova and Polikarpov, 2003). Incorporation of ^{15}N into the 2-10 cm depths increased relatively slowly thereafter but resulted in higher downward transport in the nutrient amended treatments as the incubations progressed (average over 3.5-10.5 d; ambient 15.6 ± 2.0%; minimal 22.6 ± 2.8%; moderate 23.6 ± 2.7%; and elevated 21.2 ± 2.0%, Fig. 2). Downward migration of MPB can be enhanced by light stress (Underwood 2002), but given that light intensity was consistent across treatments, the increased downward transfer of MPB-N within the nutrient amended treatments more likely reflects increased downward migration for nutrients and mitosis as water column nutrients quickly became limiting later in the incubations (Saburova and Polikarpov, 2003).

4.2 *Transfer of MPB-N within sediments*

The transfer and processing of MPB-N within the sediment compartments varied between the ambient and nutrient amended treatments, potentially as a result of tight coupling between bacterial remineralization and EPS production by MPB providing efficient recycling and transfer of MPB-N between all sediment compartments within sediment ON (Fig. 5). In the ambient treatment, as the incubation progressed, the contribution of MPB to ^{15}N within microbial biomass increased (77-90%), bacterial contributions declined (10-23%, Fig. 3), and the uncharacterized pool of ^{15}N contributed considerably to the excess ^{15}N in sediment ON (23-61%, Fig. 3). These combined factors suggest that MPB-N is efficiently recycled when nutrients are relatively scarce. Bacteria in the ambient treatment likely re-mineralized MPB-N within the uncharacterized pool (Fig. 1A), providing inorganic nutrients that were increasingly used by MPB they competed for available nutrients under nutrient limitation (Cook et al., 2007).

564 In contrast, as incubations progressed in the nutrient amended treatments, decoupling
565 between MPB and recycled nutrients from bacterial remineralization likely resulted in
566 accumulation of ^{15}N within sediment ON as MPB-N was not utilized by bacteria and quickly
567 recycled. With increased nutrient loading, MPB contributions to ^{15}N within microbial
568 biomass declined, bacterial contributions increased (Fig. 3), and coincided with an increased
569 contribution of ^{15}N to the uncharacterized pool (minimal, 41-47%; moderate 29-75%;
570 elevated 23-70%; Fig. 3). The accumulation of ^{15}N in the uncharacterized sediment
571 compartment reflects decreased recycling of MPB-N contained in EPS and detritus (derived
572 from MPB and bacterial biomass) as bacteria preferentially utilize inorganic nutrients instead
573 of MPB-N within the uncharacterized pool (Fig. 1B). The increased contribution of bacteria
574 to the microbial community largely reflects increased turnover of ^{15}N out of MPB as
575 increased production shunts MPB-N into the uncharacterized pool.

576 4.3 *Effluxes of MPB-N*

577 Export of ^{15}N from the sediments to the water column primarily occurred via fluxes
578 of DON, N_2, and NH_4^+ (Fig. 2 & 16). Fluxes of NH_4^+ resulting from remineralization (0-
579 0.3%) contributed little to the export of ^{15}N across all treatments, indicating strong retention
580 of nutrients arising from MPB-N remineralization. Strong retention of this N is not
581 unexpected, as competition between MPB and heterotrophic bacteria for N has been
582 previously observed under nutrient limiting settings (Agogue et al., 2014). Limited export of
583 ^{15}N as NH_4^+ across all treatments in this study suggests that the microbial community
584 maintained capacity for further N uptake throughout the incubations. The cumulative flux of
585 NH_4^+ observed in this study was considerably smaller than that observed in subtropical
586 subtidal sediments over 33 d (20.8%, Eyre et al. 2016) but was comparable to that found

587 previously for this site across 31 d (0.2%, Oakes et al. in press). These comparable fluxes are
588 likely due to the decreased bacterial remineralization and increased retention of MPB-N that
589 was observed within this study.

590 Low fluxes of N_2 may also relate to the competition for inorganic nutrients between
591 MPB and bacteria. The intense competition for recycled inorganic nutrients between MPB
592 and bacteria would have starved denitrifying bacteria of NO_3^- (McGlathery et al., 2007;
593 Sundbäck and Miles, 2002) and greatly reduced the amount of N_2 efflux from denitrification
594 (2.3-7.1%, 10.5 d; Fig. 6). This finding is comparable with previously reported
595 denitrification rates reported for this site (2.6% by 31 d; Oakes et al. in press), and suggests
596 that competition from MPB for NH_4^+ was similarly limiting during that period as ambient
597 NH_4^+ was higher in Oakes et al. in press (2.1±1.8 $\mu molL^{-1}$) than observed in this study
598 (0.9±0.1 $\mu molL^{-1}$). Limited availability of NO_3^- required for denitrification due to intense
599 competition for the substrate for nitrification would help to explain the low N_2 efflux
600 observed within this study compared to that found previously for this site as well as in
601 subtropical subtidal sediments (20.7%, Eyre et al. (2016). The enhanced efflux of MPB-N as
602 both N_2 and NH_4^+ that was previously observed in a subtidal subtropical setting (20.7% N_2
603 and 20.8% NH_4^+, Eyre et al. 2016a versus 2.3-7.1% N_2 and 0.02-0.09% NH_4^+, this study;
604 Figs. 3 & 6) suggests that remineralization produced inorganic nutrients in excess of what
605 was required by the microbial community in that system and resulted in increased export of
606 ^{15}N via DIN and denitrification.

607 Within the current study, increased inorganic nutrient availability appeared to
608 decouple remineralization of MPB-N by bacteria as inorganic nutrients were preferentially

609 utilized instead of sediment ON (Fig. 1B). In the ambient treatment, efflux of MPB-N via
610 DON accounted for 10% of the ^{15}N assimilated within the system and is evidence of
611 considerable remineralization, hydrolysis of freshly deposited material (Ferguson et al.,
612 2004), and export of MPB-N from the uncharacterized pool within sediment ON. With
613 nutrient amendment, export of MPB-N via DON decreased to 3.9-5.2% (Fig. 6) and occurred
614 despite enhanced MPB-N production and the equal or increased presence of ^{15}N within the
615 uncharacterized pool within the nutrient amended treatments. This indicates that bacteria
616 preferentially utilized inorganic nutrients instead of MPB-N derived from ^{15}N-labeled EPS
617 contained within the uncharacterized sediment pool, likely as a result of preferential
618 remineralization of other non-labeled EPS or organic matter that is present in the sediments.

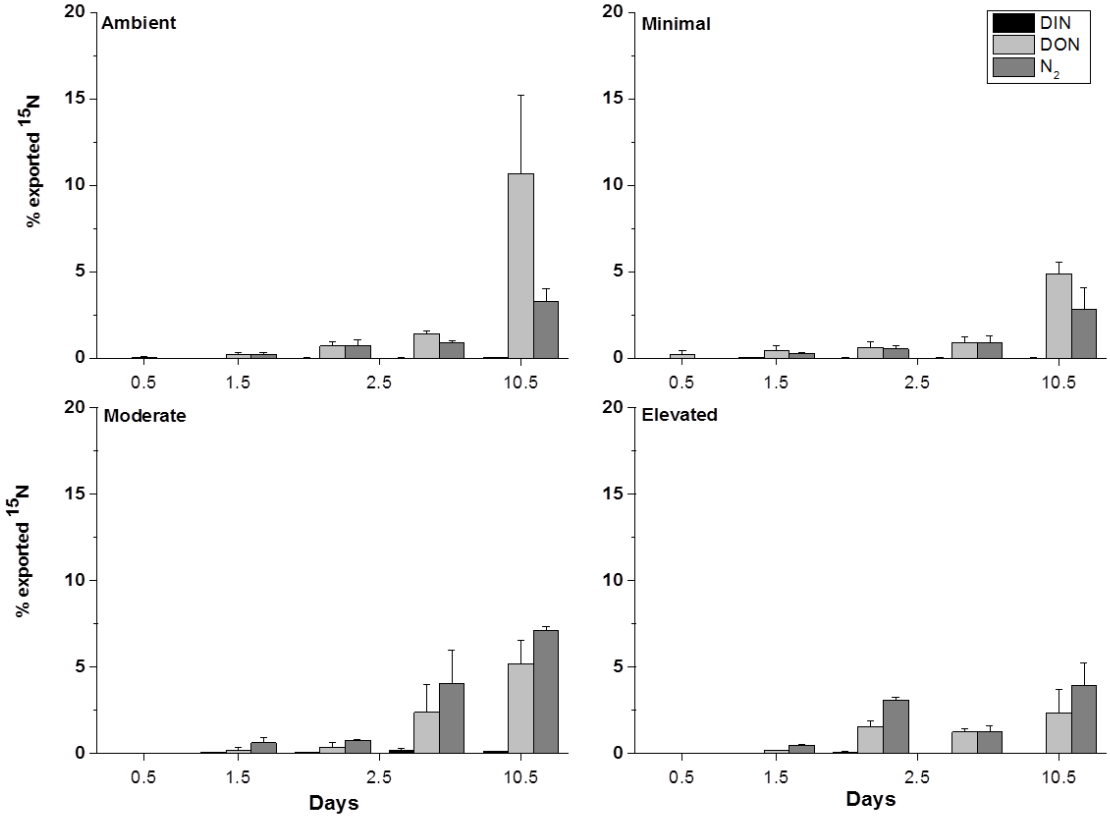

Figure 5: Cumulative excess ^{15}N lost via efflux of DIN, DON, and N_2 at each sampling time. All values are as a percentage of the ^{15}N incorporated into sediment ON (0-10 cm). Some bars and error bars are too small to be seen (mean + SE).

4.4 *Retention of MPB-N*

MPB have a considerable role in regulating the processing of nutrients within shallow unvegetated benthic settings through primary production and N uptake (Ferguson and Eyre, 2013; Ferguson et al., 2004; McGlathery et al., 2007; Nielsen et al., 2017; Sundbäck and Miles, 2002). Newly assimilated N has been typically considered to be retained within MPB biomass, with increased MPB biomass resulting in reduced N efflux from sediments (Sundbäck et al., 2006). Excluding Eyre et al. (2016) and Oakes et al. (in

press), previous studies have not used biomarkers to partition sediment ON into compartments representing the contributions from microbial groups (MPB, bacteria) as well as processed MPB-N remaining in the sediment (uncharacterized). Partitioning out the uncharacterized pool within sediment ON reveals that much of the initially assimilated MPB-N is transferred into the uncharacterized pool, presumably via excretion of EPS by MPB and turnover of microbial cellular material. Under nutrient-limiting conditions, this EPS is quickly remineralized by bacteria, releasing $^{15}NH_4^+$ that is then recycled as MPB and bacteria compete for available nutrients (Fig. 1A). Under ambient conditions, this coupling resulted in efficient recycling of MPB-N and caused considerable turnover of ^{15}N between the uncharacterized, MPB and bacteria sediment compartments, although sediment retention was somewhat reduced by increased efflux of DON through increased hydrolysis and bacterial remineralization of freshly deposited MPB-N. When nutrient amendments were added, hydrolysis and bacterial remineralization of MPB-N appeared to slow, resulting in reduced processing and accumulation of MPB-N within sediment ON and decreased loss of ^{15}N via DON efflux. The net result of these changes is increased retention of MPB-N under nutrient amendment, as processing and export of assimilated N is reduced. Where MPB-N was retained it was largely contained outside of the microbial biomass, largely within the uncharacterized sediment ON pool (i.e., it was retained as EPS and other N-containing molecules). This is in stark contrast to previous findings that MPB-N is predominately strongly retained in MPB-biomass (Eyre et al., 2016; Nielsen et al., 2017) and likely reflects the considerable turnover of MPB-N within this system.

5 Conclusion

652 The microbial community is an important sink for both organic and inorganic N
653 within benthic coastal settings (Ferguson et al., 2004; McGlathery et al., 2007; Thornton et
654 al., 2002). Uptake of N is typically viewed as being MPB dominated, with N predominately
655 retained in MPB biomass (Evrard et al., 2008; Hardison et al., 2011; Sundbäck et al., 2006;
656 Veuger et al., 2007a) unless grazing leads to trophic transfer of MPB-N. The addition of
657 inorganic nutrients appears to initially stimulate incorporation of N into MPB, but then leads
658 to decoupling between bacterial remineralization and production of MPB-N as inorganic
659 nutrients are utilized to drive breakdown of other non-labeled organic matter. This leads to
660 decreased MPB-N retention within MPB biomass, greater accumulation of MPB-N within
661 sediment ON as uncharacterized material and corresponds with decreased efflux of MPB-N
662 as DON. This material is composed of a mixture of EPS, enzymes and other N-bearing OM
663 that is either associated with the biofilm formed by MPB and bacteria and fairly resistant to
664 export or has accumulated due to the low physical transport processes associated with this
665 study. In either case, turnover of MPB-N between the sediment compartments has decreased,
666 with MPB-N being less efficiently recycled, and no longer strongly solely retained within
667 MPB biomass. The net effect of these changes appears to be increased presence of relatively
668 labile MPB-N in the shallow surface sediments which may lead to longer term support of
669 increased bacterial respiration. If MPB production slows, there is potential to shift the
670 benthic metabolism from net autotrophy towards net heterotrophy.

671

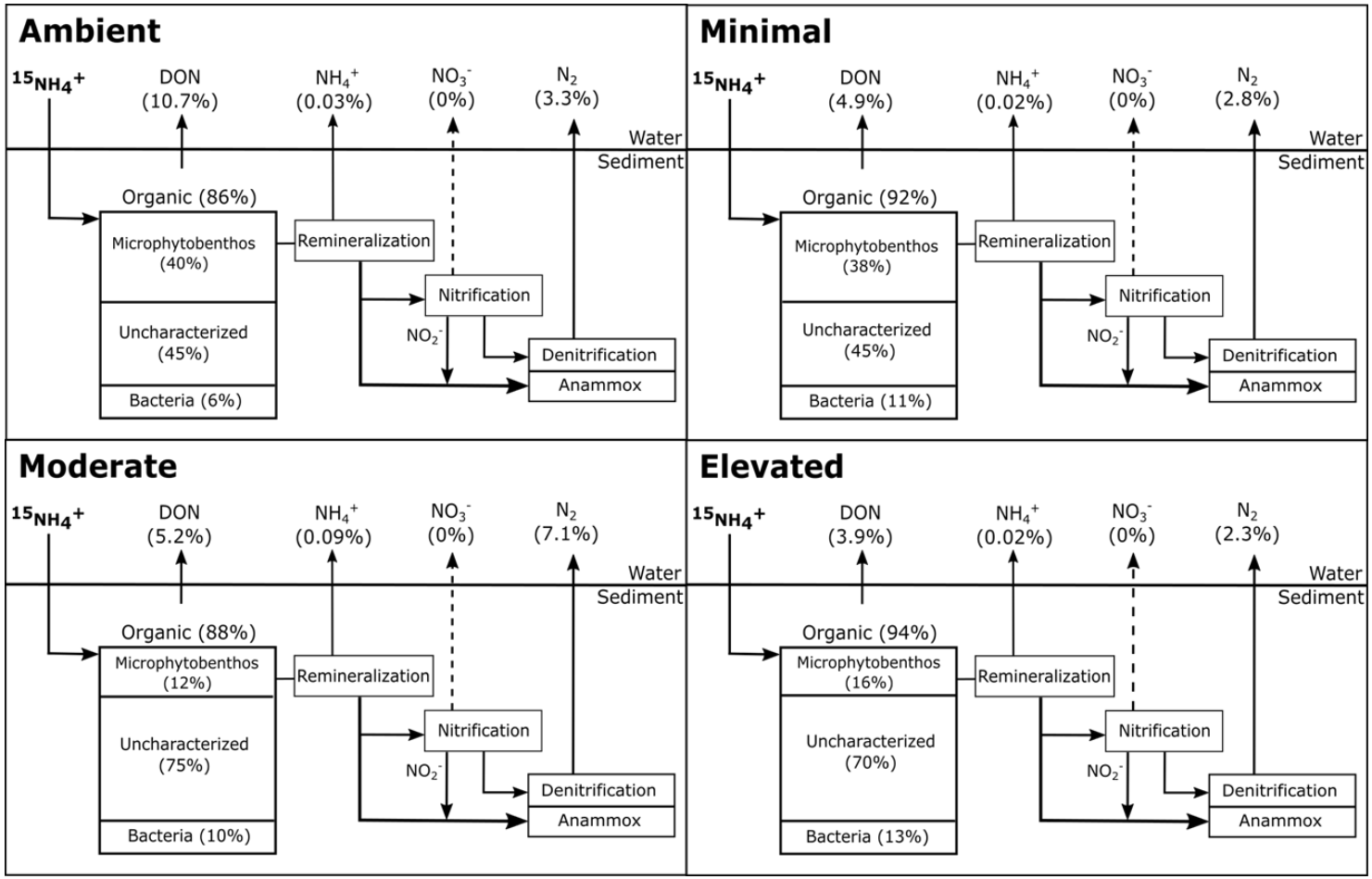

672

673 **Figure 6: Conceptual model comparing the processing and fate of microphytobenthos nitrogen after 10.5 d of incubation**
674 **amongst treatments. Sediment organic nitrogen is partitioned into sediment compartments (microphytobenthos, bacteria, and**
675 **uncharacterized) as a percentage of ^{15}N contained in 0-10 cm depth using biomarker analyses for 0-2 cm, 2-5 cm, and 5-10 cm**
676 **depths. The dashed line for efflux of NO_3^- indicates that concentrations were consistently below the detection limit for $^{15}NO_3^-$**
677 **analysis (figure modified from Eyre et al. 2016)**

Acknowledgements

We thank Natasha Carlson-Perret and Jessica Riekenberg for field assistance, Iain Alexander for laboratory analysis, and Matheus Carvalho for isotope analysis. This study was funded by an Australian Research Council (ARC) Linkage Infrastructure, Equipment and Facilities grant to B.D.E. (LE0668495), an ARC Discovery Early Career Researcher Award to J.M.O. (DE120101290), an ARC Discovery grant to B.D.E. (DP160100248), and ARC Linkage Grants to B.D.E. (LP110200975; LP150100451; LP150100519).

References

Agogue H., Mallet C., Orvain F., De Crignis M., Mornet F., Dupuy C. (2014) Bacterial dynamics in a microphytobenthic biofilm: A tidal mesocosm approach. *Journal of Sea Research* **92**, 36-45.

Cook P.L.M., Revill A.T., Butler E.C.V., Eyre B.D. (2004) Carbon and nitrogen cycling on intertidal mudflats of a temperate australian estuary. Ii. Nitrogen cycling. *Marine Ecology Progress Series* **280**, 39-54.

Cook P.L.M., Veuger B., Boer S., Middelburg J.J. (2007) Effect of nutrient availability on carbon and nitrogen and flows through benthic algae and bacteria in near-shore sandy sediment. *Aquatic Microbial Ecology* **49**, 165-180.

Dalsgaard T. (2003) Benthic primary production and nutrient cycling in sediments with benthic microalgae and transient accumulation of macroalgae. *Limnology and Oceanography* **48**, 2138-2150.

Erler D.V., Wang X.T., Sigman D.M., Scheffers S.R., Shepard B.O. (2014) Control on the nitrogen isotopic composition of shallow water corals across a tropical reef flat transect. *Coral Reefs* **34**, 329-338.

Evrard V., Cook P.L.M., Veuger B., Huettel M., Middelburg J.J. (2008) Tracing carbon and nitrogen incorporation and pathways in the microbial community of a photic subtidal sand. *Aquatic Microbial Ecology* **53**, 257-269.

Eyre B. (1997) Water quality changes in an episodically flushed sub-tropical australian estuary: A 50 year perspective. *Marine Chemistry* **59**, 177-187.

Eyre B., Ferguson A.P., Webb A., Maher D., Oakes J. (2011) Denitrification, n-fixation and nitrogen and phosphorus fluxes in different benthic habitats and their contribution to the nitrogen and phosphorus budgets of a shallow oligotrophic sub-tropical coastal system (southern moreton bay, australia). *Biogeochemistry* **102**, 111-133.

Eyre B., Oakes J.M., Middelburg J.J. (2016) Fate of microphytobenthos nitrogen in subtropical sediments: A ^{15}n pulse-chase study. *Limnology and Oceanography* **61**, 1144-1156.

Eyre B.D. (2000) Regional evaluation of nutrient transformation and phytoplankton growth in nine river-dominated sub-tropical east australian estuaries. *Marine Ecology Progress Series* **205**, 61-83.

Eyre B.D., Rysgaard S., Dalsgaard T., Christensen P.B. (2002) Comparison of isotope pairing and n2:Ar methods for measuring sediment denitrification—assumption, modifications, and implications. *Estuaries* **25**, 1077-1087.

715 Ferguson A., Eyre B. (2013) Interaction of benthic microalgae and macrofauna in the control of benthic
716 metabolism, nutrient fluxes and denitrification in a shallow sub-tropical coastal embayment
717 (western moreton bay, australia). *Biogeochemistry* **112**, 423-440.
718 Ferguson A.J.P., Eyre B.D., Gay J.M. (2003) Organic matter and benthic metabolism in euphotic
719 sediments along shallow sub-tropical estuaries, northern new south wales, australia. *Aquatic*
720 *Microbial Ecology* **33**, 137-154.
721 Ferguson A.J.P., Eyre B.D., Gay J.M. (2004) Benthic nutrient fluxes in euphotic sediments along shallow
722 sub-tropical estuaries, northern new south wales, australia. *Aquatic Microbial Ecology* **37**, 219-
723 235.
724 Forehead H., Thomson P., Kendrick G.A. (2013) Shifts in composition of microbial communities of
725 subtidal sandy sediments maximise retention of nutrients. *FEMS Microbiology Ecology* **83**, 279-
726 298.
727 Goldman J.C., Dennett M.R. (2000) Growth of marine bacteria in batch and continuous culture under
728 carbon and nitrogen limitation. *Limnology and Oceanography* **45**, 789-800.
729 Hardison A., Anderson I., Canuel E., Tobias C., Veuger B. (2011) Carbon and nitrogen dynamics in shallow
730 photic systems: Interactions between macroalgae, microalgae, and bacteria. *Limnology and*
731 *Oceanography* **56**, 1489-1503.
732 Howarth R.W., Marino R. (2006) Nitrogen as the limiting nutrient for eutrophication in coastal marine
733 ecosystems: Evolving views over three decades. *Limnology and Oceanography* **51**, 364-376.
734 Kaiser K., Benner R. (2005) Hydrolysis-induced racemization of amino acids. *Limnology and*
735 *Oceanography: Methods* **3**, 318-325.
736 Lachat. (1994) International methods list for the quickchem automated ion analyzer. Lachat
737 Instruments, Milwaukee, WI
738 Lorenzen C. (1967) Determinations of chlorophyll and peopigments: Spectrophotometric equations.
739 *Limnology and Oceanography* **12**, 343-346.
740 Madigan M.T., Martinko J.M., Parker J. (2000) Brock biology of microorganisms, 9th ed., Prentice-Hall
741 McGlathery K.J., Sundbäck K., Anderson I.C. (2007) Eutrophication in shallow coastal bays and lagoons:
742 The role of plants in the coastal filter. *Marine Ecology Progress Series* **348**, 1-18.
743 McKee L.J., Eyre B.D., Hossain S. (2000) Transport and retention of nitrogen and phosphorus in the sub-
744 tropical richmond river estuary, australia: A budget approach. *Biogeochemistry* **50**, 241-278.
745 Middelburg J.J., Nieuwenhuize J. (2001) Nitrogen isotope tracing of dissolved inorganic nitrogen
746 behaviour in tidal estuaries. *Estuarine, Coastal and Shelf Science* **53**, 385-391.
747 Nielsen S.L., Risgaard-Petersen N., Banta G.T. (2017) Nitrogen retention in coastal marine sediments—a
748 field study of the relative importance of biological and physical removal in a danish estuary.
749 *Estuaries and Coasts*, 1-12.
750 Oakes J.M., Eyre B., D., Middelburg J.J. (2012) Transformation and fate of microphytobentos carbon in
751 subtropical shallow subtidal sands: A ^{13}c-labeling study. *Limnology and Oceanography* **57**, 1846-
752 1856.
753 Oakes J.M., Eyre B.D. (2014) Transformation and fate of microphytobenthos carbon in subtropical,
754 intertidal sediments: Potential for long-term carbon retention revealed by 13c-labeling.
755 *Biogeosciences* **11**, 1927-1940.
756 Oakes J.M., Rysgaard S., Glud R.N., Eyre B.D. (2016) The transformation and fate of sub-arctic
757 microphytobenthos carbon revealed through ^{13}c-labeling. *Limnology and Oceanography*, 2296-
758 2308.
759 Oakes J.M., Riekenberg P.M., Eyre B.D. (In Press) Fate of intertidal microphytobenthos nitrogen under
760 enhanced nutrient availability: Evidence for reduced nitrogen retention revealed through ^{15}N-
761 labeling. *Limnology and Oceanography*: 10.1002/lno.11459

762 Rabalais N.N., Turner R.E., Díaz R.J., Justić D. (2009) Global change and eutrophication of coastal waters.
763 *ICES Journal of Marine Science* **66**, 1528-1537.
764 Riekenberg P.M., Oakes J.M., Eyre B.D. (2017) Uptake of dissolved organic and inorganic nitrogen in
765 microalgae-dominated sediment: Comparing dark and light *in situ* and *ex situ* additions of ^{15}n.
766 *Marine Ecology Progress Series* **571**, 29-42.
767 Riekenberg P.M., Oakes J.M., Eyre B.D. (2018) Short-term fate of intertidal microphytobenthos carbon
768 under enhanced nutrient availability: A ^{13}c pulse-chase experiment. *Biogeosciences* **15**, 2873-
769 2889.
770 Saburova M.A., Polikarpov I.G. (2003) Diatom activity within soft sediments: Behavioural and
771 physiological processes. *Marine Ecology Progress Series* **251**, 115-126.
772 Sigman D.M., Casciotti K.L., Andreani M., Barford C., Galanter M., Bohlke J.K. (2001) A bacterial method
773 for the nitrogen isotopic analysis of nitrate in seawater and freshwater. *Analytical Chemistry* **73**,
774 4145-4153.
775 Sundbäck K., Miles A. (2002) Role of microphytobenthos and denitrification for nutrient turnover in
776 embayments with floating macroalgal mats: A spring situation. *Aquatic Microbial Ecology* **30**, 91-
777 101.
778 Sundback K., Miles A., Goransson E. (2000) Nitrogen fluxes, denitrification and the role of
779 microphytobenthos in microtidal shallow-water sediments: An annual study. *Marine Ecology*
780 *Progress Series* **200**, 59-76.
781 Sundbäck K., Miles A., Linares F. (2006) Nitrogen dynamics in nontidal littoral sediments: Role of
782 microphytobenthos and denitrification. *Estuaries and Coasts* **29**, 1196-1211.
783 Thornton D.C.O., Dong L.F., Underwood G.J.C., Nedwell D.B. (2002) Factors affecting microphytobenthic
784 biomass, species composition and production in the colne estuary (uk). *Aquatic Microbial Ecology*
785 **27**, 285-300.
786 Valderrama J. (1981) The simultaneous analysis of tp and tn in natural waters. *Marine Chemistry* **10**,
787 109-122.
788 Van den Meersche K., Middelburg J.J., Soetaert K., Rijswijk P.v., Boschker H.T.S., Heip C. (2004) Carbon-
789 nitrogen coupling and algal-bacterial interactions during an experimental bloom: Modeling a ^{13}c
790 tracer experiment. *Limnology and Oceanography* **49**, 862-878.
791 Veuger B., Eyre B., D., Maher D., Middelburg J.J. (2007a) Nitrogen incorporation and retention by
792 bacteria, algae, and fauna in a subtropical intertidal sediment: An in situ ^{15}n-labeling study.
793 *Limnology and Oceanography* **52**, 1930-1942.
794 Veuger B., Middelburg J.J., Boschker H.T.S., Houtekamer M. (2005) Analysis of ^{15}n incorporation into d-
795 alanine: A new method for tracing nitrogen uptake by bacteria. *Limnology and Oceanography:*
796 *Methods* **3**, 230-240.
797 Veuger B., Middelburg J.J., Boschker H.T.S., Houtekamer M. (2007b) Update of "analysis of 15n
798 incorporation into d-alanine: A new method for tracing nitrogen uptake by bacteria" *Limnology*
799 *and Oceanography: Methods* **5**, 192-194.
800 Zhang L., Altabet M.A., Taixing W., Hades O. (2007) Sensitive measurement of nh_4^+ ^{15}n/^{14}n ($\delta^{15}nh_4^+$) at
801 natural abundance levels in fresh and saltwaters. *Analytical Chemistry* **79**, 5297-5303.

802

803

804

805

806

807 Appendix

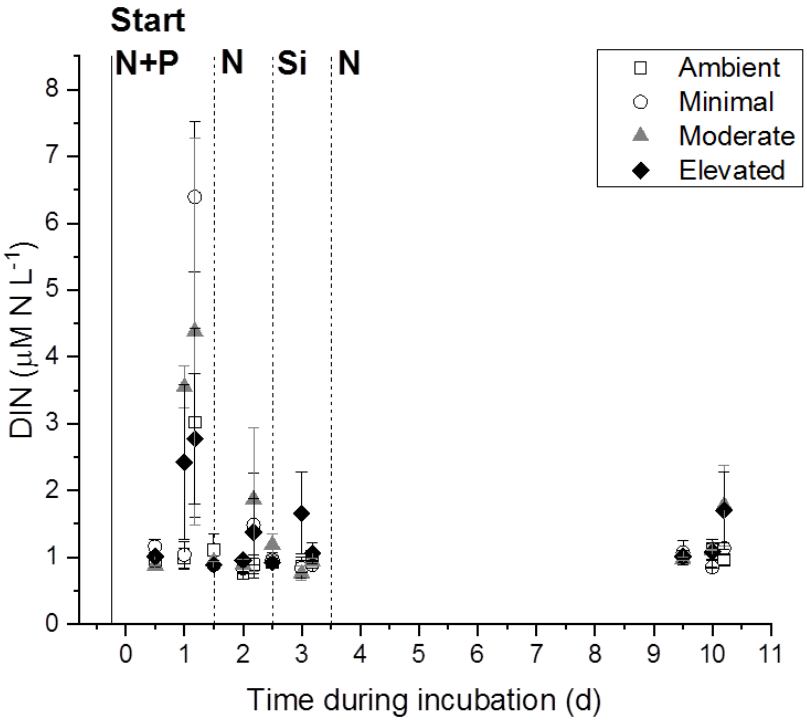

808

809 **Appendix Figure 1:** Dissolved inorganic nitrogen in the overlying core waters during sampling
810 for light and dark incubations. The y-axis intercept represents the initial application of $^{15}NH_4^+$ to
811 the sediment. The solid line is when cores were placed into treatment tanks prior to the start of
812 incubation. Dashed lines represent additional treatment pulses ($N=NH_4^+$, $P=PO_4^{3-}$, $Si=SiO_3$) that
813 occurred during incubation.